

WHAT DOES THE INTERPLANETARY HYDROGEN TELL US ABOUT THE HELIOSPHERIC INTERFACE ?

F. E. Vincent¹, L. Ben-Jaffel¹ and W. M. Harris²

Abstract. The heliospheric interface results from the interaction between the solar wind and the local interstellar medium (LISM). The interplanetary hydrogen (IPH), a population of neutrals that fill the space between planets inside the heliosphere, carries the signature of the LISM and the heliospheric interface: as the incoming ISM ionized component deflects at the heliopause, charge exchange reactions decelerate the bulk motion of the neutrals that penetrate the heliosphere. Inside the heliosphere, the IPH is further affected by the Sun and resonantly scatters the solar Lyman-alpha photons. Solar cycle 23 provided the first partial temporal map of the IPH velocity. We present an updated analysis of IPH velocity measurements from *Hubble Space Telescope* spectrometers (Goddard High Resolution (GHRS) and Space Telescope Imaging Spectrograph (STIS)) and compare these results with those of the *Solar and Heliospheric Observatory* (SOHO)/Solar Wind ANisotropies (SWAN) instrument and two different time-dependent models. With updates to the HST data points, we now find that all data can be fit by the existing models to within 1σ , with the exception of SWAN observations taken at solar minimum (1997/98). We interpret this discrepancy as a possible effect due to the obliquity of the local interstellar magnetic field. New observations are required to determine the detailed characteristics of the solar cycle dependence and to monitor the possible changes in the LISM parameters as recently reported by the *Interstellar Boundary Explorer* (IBEX) spacecraft.

Keywords: Ultraviolet: stars, interplanetary medium, Sun: heliosphere, ISM: general

1 Introduction

The Solar system is moving through the Local Interstellar Cloud, a diffuse warm and partially ionized medium, mainly composed of atomic hydrogen (Frisch 2009). The fundamental aspect of the interaction between the solar wind (SW) and the local interstellar medium (LISM) is the dynamic equilibrium between two counter-flowing magnetized plasmas that meet and are separated along a tangential discontinuity, the heliopause (Parker 1961; Baranov et al. 1971; Axford 1972). The overall shape and location of the heliopause is determined by the relative velocity of the solar wind and LISM and the plasma densities on either side of the barrier. In the generalized model of the interaction, the SW and the ionized LISM are decelerated to subsonic speeds through shocks that are respectively located inside (the termination shock) and outside (the bow shock) the heliopause, as shown in figure 1. However recent observations from the *Interstellar Boundary Explorer* (IBEX) spacecraft show that the relative motion of the Sun with respect to the LISM is currently slower (23.2 ± 0.3 km/s, McComas et al. (2012)) than previously measured (~ 26 km/s) by Doppler triangulation (Bertin et al. 1993) and the *Ulysses* spacecraft (Witte et al. 1993), so almost certainly slower than the fast magnetosonic speed, which would prevent the formation and the existence of the bow shock ahead of the heliosphere.

Because of a large mean free path, a fraction of interstellar hydrogen atoms penetrates inside the heliosphere without any interaction with the interface (Blum & Fahr 1970), forming the primary population of the interplanetary hydrogen (IPH). Early space based studies of the sky background confirmed the presence of the incoming hydrogen flow (Bertaux & Blamont 1971; Thomas & Krassa 1971). Subsequent UV spectroscopic and imaging experiments provided limited access to the IPH velocity distribution (Bertaux et al. 1976, 1985; Adams & Frisch 1977; Clarke et al. 1984, 1995) and revealed a deceleration of the hydrogen flow relative to the LISM (Bertin et al. 1993).

¹ Institut d'Astrophysique de Paris, CNRS-UPMC, 98 bis, Boulevard Arago, 75014 Paris, France

² Department of Mechanical and Aerospace Engineering, University of California, One Shields Avenue, Davis, CA 95616, USA

The observed neutral LISM deceleration is believed to be traceable to the fraction of interstellar hydrogen atoms that interact with the slowing LISM protons through resonance charge exchange reactions (Wallis 1975; Ripken & Fahr 1983). These reactions result in the formation of a secondary population with a slower bulk motion, leading to the formation of a "Hydrogen Wall" between the bow shock and the heliopause, as predicted by Baranov & Malama (1993) and then observed by Linsky & Wood (1996) with observations of absorption lines in the direction of α Centauri. By contrast, interstellar helium atoms are barely affected by the heliospheric interface because of a smaller cross-section for charge-exchange reactions, and carry the signature of the LISM inside the heliosphere (Moebius et al. 2004). Observations with the Solar Wind ANisotropies (SWAN) instrument on the *Solar Wind Heliospheric Observatory (SOHO)* showed that the hydrogen flow is slightly deflected by respect to the helium flow (Lallement et al. 2005, 2010).

During the last two decades, *SOHO*/SWAN and the echelle modes of the Goddard High Resolution Spectrograph (GHRS) and Space Telescope Imaging Spectrograph (STIS) on the *Hubble Space Telescope (HST)* have been used to measure the Ly- α Doppler shift with respect to the heliospheric referential and line profile with greater precision than previous observations (Clarke et al. 1998; Scherer et al. 1999; Ben-Jaffel et al. 2000; Quémerais et al. 2006).

Within the heliosphere, the IPH velocity is affected by several temporally dependent processes related to the solar wind and solar Ly- α intensity. The Warsaw group (Rucinski & Bzowski 1995; Bzowski et al. 1997) developed a time-dependent hot model of the inner heliosphere that predicts a ~ 5 km/s modulation in IPH bulk velocity due to solar cycle changes in radiation pressure and ionization rates. More recently, fluid-kinetic models included the effects of non-stationary solar wind ram pressure on the heliospheric interface (Izmodenov & Malama 2004; Izmodenov et al. 2008; Pogorelov et al. 2010). The use of a radiative transfer model allows more precise predictions of the interplanetary background line-shifts (Scherer et al. 1999; Quémerais et al. 2008). These models all converge toward a general finding that the IPH velocity should vary by 3-4 km/s over the solar cycle, but they reach different conclusions about the rate of this change and its precise magnitude. Based on previously published values, none of them have been able to match the data consistently across the entire solar cycle (Quémerais et al. 2008).

This paper sums up the work done by Vincent et al. (2011), providing an updated analysis of the IPH velocity measurements obtained over the solar cycle 23, in particular *HST* archival data from GHRS and STIS, which are compared to previously reported measurements from *SOHO*/SWAN and model predictions of IPH velocity variations over a solar cycle. In addition, we discuss the impact of the *IBEX* results.

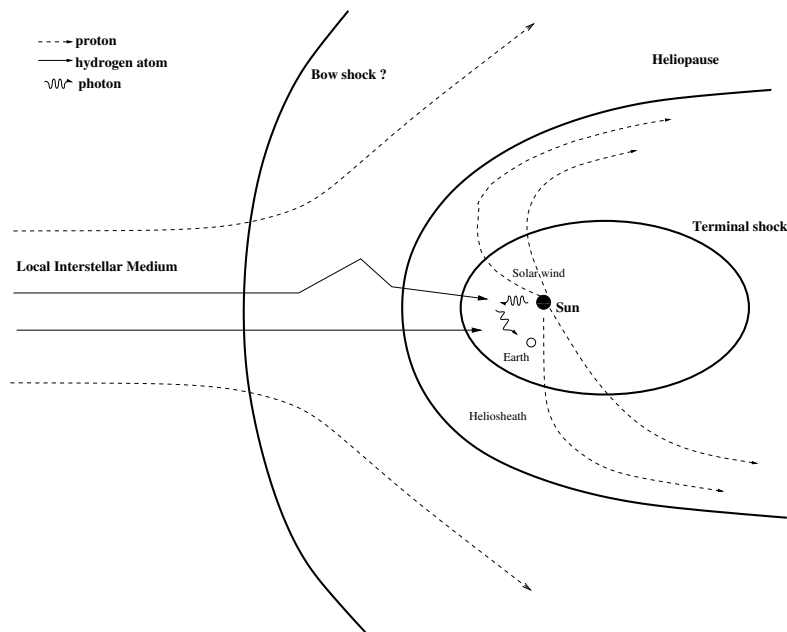


Fig. 1. Schematic of the interaction between the solar wind and the interstellar medium. The Earth's position is not to scale.

2 Data analysis

2.1 Observations

GHRs and STIS have been used to detect the backscattering of solar Ly α photons by the IPH, using the same line of sight (LOS): ($\lambda = 253.3^\circ$, $\beta = 7.0^\circ$) in ecliptic coordinates. The inner heliosphere (inside 40 AU) is dominated by solar EUV photoionization and charge exchange with SW protons, while the outer heliosphere is more affected by the heliospheric interface. Because of an increasing neutral hydrogen density with distance from the Sun, the medium can be considered as optically thin until 10 AU, but not beyond. Full attenuation of the line occurs over a large range of heliocentric distance beyond this point, with backscatter at all points contributing to the observed line shape and brightness distribution (Quémerais 2000).

GHRs data were obtained on 1994 April 7 and 1995 March 25, STIS data on 2001 March 29. At this period of the year (March-April), Earth's and IPH's velocity vectors are most directly opposite to each other, which provides a maximal Doppler shift with respect to the geocorona. STIS observations used an unsupported mode (E140H grating with the large aperture $52'' \times 0.5''$), increasing the signal from an extended source like the IPH, but resulting in blending of different orders of the echelle spectrum, as showed in Figure 2 (left).

2.2 Fitting procedure and results

GHRs and STIS spectra contain Ly α line profiles from the geocorona and the IPH, with some contamination from a geocoronal oxygen triplet line in STIS observations. Each line profile was fitted using the convolution of a Voigt profile with a measured or simulated line-spread function (LSF), and the 1σ errors were computed with $\sigma = \sqrt{\sigma_I^2 + \sigma_S^2}$, where σ_I and σ_S are respectively the instrumental and statistical uncertainties (Vincent et al. 2011). The line-shift of the IPH along the line of sight is derived from the Doppler shift between the line centers of the geocorona and the IPH, after subtraction of the velocity of the Earth along the line of sight.

Figure 2 (right) shows the fit for STIS observations. The IPH feature in the 346th order is contaminated by the 1302.168 Å O I line, so only the 347th order was used to derive the IPH line-shift. Our best fit to the STIS observations takes into account the contamination of the geocorona on the red side by the O I lines, and provides a line-shift of 22.4 ± 0.4 km/s in 2001. GHRs spectra were extracted using the existing pipeline. After fitting the lines with MPFIT and PAN, we obtained line-shifts of 24.0 ± 0.9 km/s in 1995 and 22.2 ± 1.5 km/s in 1994 (Figures 6 and 7 in Vincent et al. (2011)). The subsection 3.1. in Vincent et al. (2011) makes a comparison of this work with previous analyses of HST data.

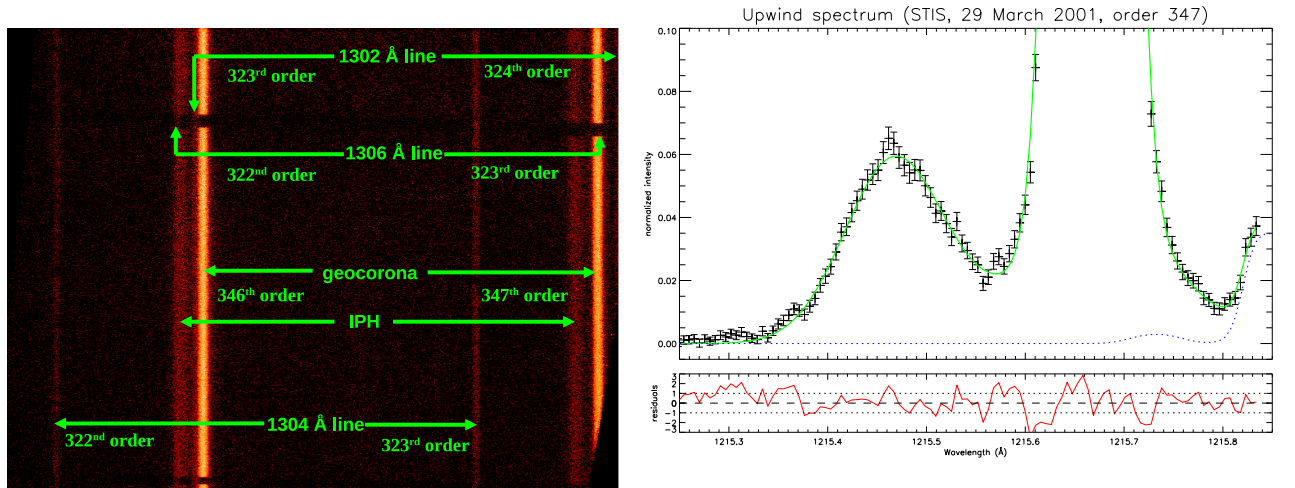


Fig. 2. Left: STIS spectro-image from observations made on 29 March 2001, after correction of the geometric distortion. The Ly- α emission from IPH and geocorona is transmitted by two orders (346 and 347) but suffers from contamination by geocoronal oxygen emission lines. The central line of the O I triplet (1304.858 Å) is isolated and clearly visible. Both other lines (1302.168 and 1306.029 Å) overlap with the Ly- α emission but appear at the location of the occulting bars where the Ly- α emission is blocked. **Right:** Fitting of STIS observations for the order 347. The blue dotted lines represent the contaminations by oxygen lines: 1306.029 Å (order 323) and 1302.168 Å (order 324), from left to right.

3 Discussion

3.1 Comparison with SWAN data and models

Quémerais et al. (2006) derived interplanetary Ly- α line profiles from annually averaged observations made by the SWAN instrument. Their findings indicate a velocity change from 25.7 ± 0.2 km/s to 21.4 ± 0.5 km/s in the solar rest frame between 1997 and 2003.

Figure 3 plots the IPH velocities found by this work for GHRs & STIS observations, and by Quémerais et al. (2006) for SWAN data and STIS observations. In order to show the possible solar cycle effect, we over-plotted the predictions of the physically realistic models developed by Quémerais et al. (2008) and Scherer et al. (1999) (noted Q2008 and S1999 respectively).

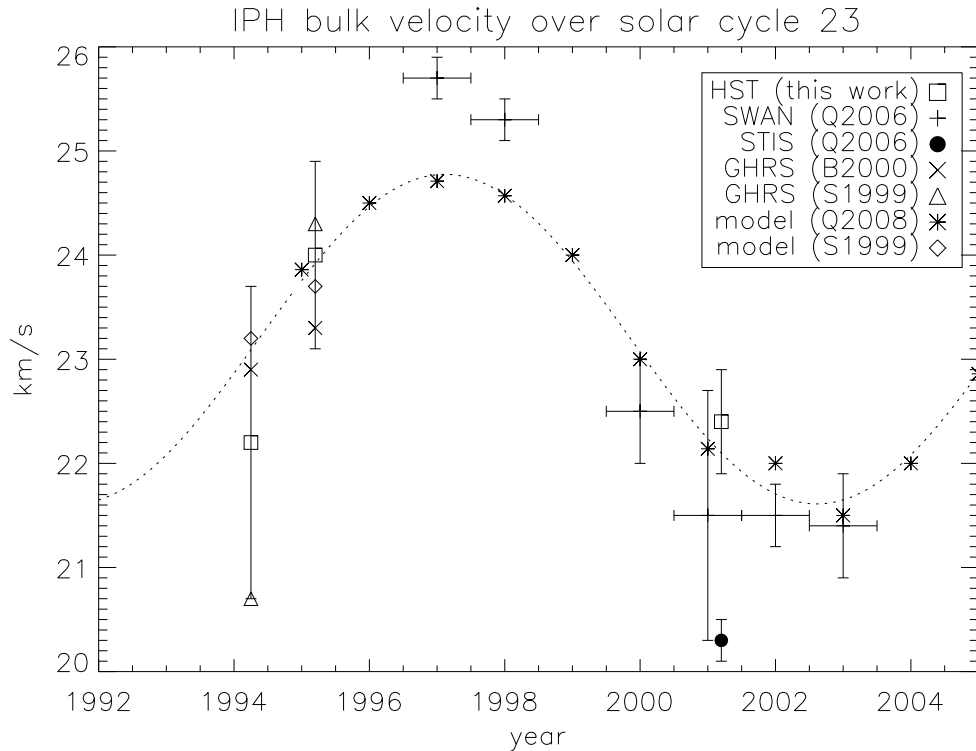


Fig. 3. IPH bulk velocity in the upwind direction over solar cycle 23, with values reported by this work (squares for GHRs and STIS), by Quémerais et al. (2006) (plus signs for SWAN data, filled circle for STIS observations), by Ben-Jaffel et al. (2000) (crosses) and Scherer et al. (1999) (triangles). The dotted curve is a Fourier interpolation of the model proposed by Quémerais et al. (2008) (asterisks). The values predicted by the model of Scherer et al. (1999) are represented with diamonds.

Compared to the value obtained by Quémerais et al. (2006), the updated STIS data reduction provides an IPH velocity that is more consistent with SWAN data and the Q2008 model for the period near solar maximum (in 2001). Similarly our revised GHRs analysis provides a much better fit to the models than that provided in Scherer et al. (1999). As a consequence, all data are within or close to 1σ from Q2008 and S1999 models, at the exception of the SWAN measurements in 1997/98.

3.2 The influence of the local interstellar magnetic field

Allowing for the statistically significant fit between the data and models near solar maximum, the primary discrepancy is found at solar minimum, where the SWAN data implies a velocity more than 2σ faster than the model. Two explanations that do not exclude one another, can be proposed to account for this difference: these include possible systematic uncertainty in the SOHO-SWAN data processing and/or an incomplete description of the IPH neutrals by the fluid-kinetic models (Scherer et al. 1999; Izmodenov et al. 2008). As explained in

the subsection 3.4.1. in Vincent et al. (2011), the error bars on SWAN measurements could be larger than previously estimated.

On the other hand, the discrepancy between data and models could be also an indirect effect of the interstellar influence, notably the local interstellar magnetic field that has not been taken into account by the previous authors (Scherer et al. 1999; Izmodenov et al. 2008; Quémerais et al. 2008). Models taking into account the oblique local interstellar magnetic field (LIMF) have shown severe distortion in the shape of the heliopause (Fahr et al. 1988; Ratkiewicz & Ben-Jaffel 2002; Izmodenov et al. 2005). Ben-Jaffel et al. (2000) showed that the excess of backscattered solar Ly- α photons detected by *Voyager 1* UVS can be interpreted as a tilt of the heliosphere's nose by respect to the upwind direction, resulting from an oblique LIMF with a deviation $\sim 40^\circ$ from the interstellar flow direction. Results obtained by SWAN showed that the interstellar neutral hydrogen flow is deflected relative to the helium flow, providing new evidence for the obliquity of the LIMF (Lallement et al. 2005, 2010). More recent models can account for the 10 astronomical units (AU) difference in the TS heliospheric distances observed by the *Voyager 1* and *Voyager 2* spacecraft (Ratkiewicz & Grygorczuk 2008; Pogorelov et al. 2009; Opher et al. 2009). Even more recently, *IBEX* found a ribbon of energetic neutral atoms around the heliosphere, another proxy of the influence of the LIMF (McComas et al. 2009; Heerikhuisen et al. 2010). All observations and data analyses converge on the fact that the deviation of the LIMF from the interstellar flow direction is between 30° and 60° .

Because of the tilted nose, the density maximum will be shifted from the upwind direction as shown by most magneto-hydrodynamic and kinetic hydrogen models (Izmodenov et al. 2005; Ratkiewicz et al. 2007; Pogorelov et al. 2009). Therefore the upwind line of sight may probe regions with smaller densities and less charge exchange filtration in the outer heliosphere in the upwind direction. This weaker interaction would lead to a faster velocity component in the outer heliosphere but with a smaller weight, while the inner heliosphere component would have a bigger weight, leading to a higher IPH velocity than current models predict in the upwind direction. An oblique LIMF may thus result in a larger difference of IPH velocity (compared to IPH velocity without LIMF) at solar minimum than at solar maximum.

3.3 Need for more data

The identified issues with data near solar maximum, including the consistently low velocities obtained and the larger uncertainties, along with the discrepancy between the models and the lone data points at solar minimum, all argue for the acquisition of new data.

Moreover *IBEX* data showed that the relative motion of the Sun with respect to the LISM is currently slower (23.2 ± 0.3 km/s, McComas et al. (2012)) than previously measured (~ 26 km/s, Bertin et al. (1993); Witte et al. (1993)). There are almost 20 years between measurements, so the LISM parameters may have changed, as the Sun is moving through. Fahr et al. (1993) showed that changes in LISM over such a period may give noticeable imprints on the upwind/downwind IPH velocity distribution.

New upwind IPH observations have been recently made by *HST*/STIS and are currently being analyzed (Vincent et al. 2012). However more high-resolution measurements will be necessary to reduce the current uncertainties, better characterize the trend induced by the solar cycle, and answer the questions raised by the discrepancy at solar minimum and the possible change in the LISM parameters.

4 Conclusions

Updated analyses of both *HST*/GHRS and *HST*/STIS observations provide IPH bulk velocities of 22.2 ± 1.5 , 24.0 ± 0.9 and 22.4 ± 0.4 km/s in 1994, 1995 and 2001, respectively. These results are much more consistent with existing models. With the exception of the *SOHO*/SWAN data at 1997/98 near solar minimum, all of the data now trend within 1σ of the most physically realistic models.

In addition, the influence of the interstellar magnetic field on the heliosphere and its obliquity by respect to the interstellar flow have been proved by a multi-observational approach (*Voyager*, *SOHO*/SWAN and *IBEX*). We think that this obliquity may explain the discrepancy between models and data treating of the IPH velocity at solar minimum, and therefore it should be included in future time-dependent kinetic-fluid models.

The rather large uncertainty of some measurements near solar maximum, the discrepancy at solar minimum, and the possible change in the LISM parameters as suggested by the recent *IBEX* results, call for the acquisition of more high-resolution measurements with *HST*/STIS.

We thank Yan B  tr  mieux (MPI) for his critical feedback, as well as John Clarke (BU) for discussions about *HST* observations. We are also very grateful to the COS/STIS help desk and to Craig Markwardt (GSFC) for their help. F.E.V. and W.M.H. acknowledge support from NASA through the grant NNX08AI98G to UCD. F.E.V. and L.B.J. acknowledge support from CNES (through the INSPIRE project), CNRS and UPMC.

References

- Adams, T.F., Frisch, P. 1977, *ApJ*, 212, 300
- Axford, W. I. 1972, in *Solar Wind*, ed. C. P. Sonett, P. J. Coleman, Jr., & J. M. Wilcox (NASA SP-308), 609
- Baranov, V.B., Krasnobaev, K.V., Kulikovskii, A.G. 1971, *Soviet Phys. Doklady*, 15, 791
- Baranov, V. B., Malama, Y. G. 1993, *J. Geophys. Res.*, 98, 15157
- Bertaux, J.L., Blamont, J.E. 1971, *A&A*, 11, 200
- Bertaux, J.L., Blamont, J.E., Tabari  , N., Kurt, V.G., Bourgin, *et al.*, 1976, *A&A*, 46, 19
- Bertaux, J.L., Lallement, R., Kurt, V.G., Mironova, E.N. 1985, *A&A*, 150, 1
- Bertaux, J.L., *et al.* 1995, *Sol. Phys.*, 162, 403
- Bertin, P., Lallement, R., Ferlet, R., Vidal-Majar, A. 1993, *J. Geophys. Res.*, 98, 15193
- Ben-Jaffel, L., Puyoo, O., Ratkiewicz, R. 2000, *ApJ*, 533, 924
- Blum, P.W., Fahr, H.J. 1970, *A&A*, 4, 280
- Bzowski, M., Fahr, H.J., Rucinski, D., Scherer, H. 1997, *A&A*, 326, 396
- Clarke, J.T., Bowyer, S., Fahr, H.J., Lay, G. 1984, *A&A*, 139, 389
- Clarke, J.T., Lallement, R., Bertaux, Qu  merais, E. 1995, *ApJ*, 448, 893
- Clarke, J.T., Lallement, R., Bertaux, J.L., Fahr, H., Qu  merais, E., Scherer, H. 1998, *ApJ*, 499, 482
- Dimeo, R. *et al.* 2005, <http://www.ncnr.nist.gov/staff/dimeo/panweb/pan.html>
- Fahr H.J., Grzedzielski, S., Ratkiewicz, R. 1988, *Ann. Geophys.*, 6(4), 337
- Fahr, H.J., Rucinski, D., Judge, D.L. 1993, *A&A*, 268, 792
- Frisch, P.C. 2009, *Space Sci. Rev.*, 143, 191
- Heerikhuisen, J., *et al.* 2010, *ApJ*, 708, 126
- Izmodenov, V., Malama, Y.G. 2004, *Adv. Space Res.*, 34, 74
- Izmodenov, V., Alexashov, D., Myasnikov, A. 2005, *A&A*, 437, L35
- Izmodenov, V., Malama, Y.G., Ruderman, M.S. 2008, *Adv. Space Res.*, 41, 318
- Lallement, R., Qu  merais, E., Bertaux, J.L., Ferron, S., Koutroumpa, D., *et al.*, 2005, *Science*, 307, 1447
- Lallement, R., Qu  merais, E., Koutroumpa, D., Bertaux, J.L., Ferron, S., *et al.*, 2010, *AIP Conf. Proc.*, 1216, 555
- Linsky, J.L., Wood, B.E. 1996, *ApJ*, 463, 254
- Markwardt, C. B. 2008, *ASP Conference Series*, 411, 251
- McComas, D.J. *et al.* 2009, *Science*, 326, 959
- McComas, D.J., Alexashov, D., Bzowski, M., Fahr, H., Heerikhuisen, J., *et al.*, 2012, *Science*, 336, 1291
- Moebius, E. *et al.* 2004, *A&A*, 426, 897
- Parker, E.N. 1961, *ApJ*, 134, 20
- Opher, M., Richardson, J.D., Toth, G., Gombosi, T.I. 2009, *SSR*, 143, 43
- Pogorelov, N.V., *et al.* 2009, *Adv. Space Res.*, 44, 1337
- Pogorelov, N.V., *et al.* 2010, *ASPC*, 429, 266
- Qu  merais, E. 2000, *A&A*, 358, 353
- Qu  merais, E., Lallement, R., Bertaux, J.-L., Koutroumpa, D., Clarke, J., *et al.*, 2006, *A&A*, 455, 1135
- Qu  merais, E., Izmodenov, V., Koutroumpa, D., Malama, Y. 2008, *A&A*, 488, 351
- Ratkiewicz, R., Ben-Jaffel, L. 2002, *J. Geophys. Res.*, 107, 1007
- Ratkiewicz, R., Ben-Jaffel, L., Grygorczuk, J. 2007, *ASPC*, 385, 189
- Ratkiewicz, R., Grygorczuk, J. 2008, *Geophys. Res. Lett.*, 35, L23105
- Ripken, H.W., Fahr, H.J. 1983, *A&A*, 122, 181
- Ruci  ski, D., Bzowski, M. 1995, *A&A*, 296, 248
- Scherer, H., Bzowski, Fahr H.J., M., Ruci  ski, D. 1999, *A&A*, 342, 601
- Thomas, G.E., Krassa, R.F. 1971, *A&A*, 11, 218
- Vincent, F.E., Ben-Jaffel, L., Harris, W.M. 2011, *ApJ*, 738, 135
- Vincent, F.E., Ben-Jaffel, L., Harris, W.M., Clarke, J.T., Qu  merais, E. 2012, *in progress*
- Wallis, M. 1975, *Nature*, 254, 202
- Witte, M., Rosenbauer, H., Banaszekiewicz, M., Fahr, H. 1993, *Adv. Space Res.*, 13, (6)121